第 32 卷第 1 期
2016 年 1 月

无 机 化 学 学 报
CHINESE JOURNAL OF INORGANIC CHEMISTRY

Vol.32 No.1
153-160

2-吡啶甲醇和 1,1,1-三羟甲基乙烷混合配体七核锰配合物的合成、晶体结构与磁性

王会生* 乐 琳 潘 敏 钟文达 涂 伟 潘志权*

(武汉工程大学化学与环境工程学院,绿色化工过程教育部重点实验室,武汉 430074)

摘要: 四水合氯化锰、2-吡啶甲醇和 1,1,1-三羟甲基乙烷在乙腈里反应合成出一个七核 Mn 簇合物[$Mn^{II}_3Mn^{III}_4(Cl)_6(hmp)_6(thme)_2$]·$H_2O$·$3CH_3CN$(**1**·$H_2O$·$3CH_3CN$,hmpH 为 2-吡啶甲醇, $thmeH_3$ 为三羟甲基乙烷),并对该化合物进行 X 射线衍射单晶结构分析、元素分析、红外光谱和磁性研究。**1**·H_2O·$3CH_3CN$ 属于单斜晶系 *I*2/*a* 空间群,配合物核骨架可看成由交替的 Mn^{II}和 Mn^{III}离子形成一个六边形,而这个六边形又围绕在 1 个 Mn^{III}离子的周围,这种结构类型的配合物以前并没有报道过。磁性研究表明,化合物 **1**·H_2O 中 Mn^{III}与 Mn^{II}或 Mn^{III}与 Mn^{III}离子之间总体是铁磁性耦合的,交流磁化率研究发现该化合物有弱的频率依赖现象。

关键词: 七核 Mn 配合物; 混合螯合配体; 多齿螯合配体; 晶体结构; 磁性质

中图分类号: O614.71+1 **文献标识码**: A **文章编号**: 1001-4861(2016)01-0153-08

DOI:10.11862/CJIC.2016.012

Synthesis, Crystal Structure and Magnetic Properties of a Heptanuclear Mn Complex with 2-(Hydroxymethyl)pyridine and 1,1,1-Tris(hydroxymethyl)ethane Mixed-Ligands

WANG Hui-Sheng* YUE Lin PAN Min ZHONG Wen-Da TU Wei PAN Zhi-Quan*

(*School of Chemistry and Environmental Engineering, Wuhan Institute of Technology, Key Laboratory for Green Chemical Process of Ministry of Education, Wuhan* 430074, *China*)

Abstract: One heptanuclear Mn cluster [$Mn^{II}_3Mn^{III}_4(Cl)_6(hmp)_6(thme)_2$]·$H_2O$·$3CH_3CN$ (**1**·H_2O·$3CH_3CN$, hmpH=2-(hydroxymethyl)pyridine and $thmeH_3$=1,1,1-tris(hydroxymethyl)ethane) has been synthesized by the reaction of $MnCl_2·4H_2O$, hmpH and $thmeH_3$ in MeCN. The complex was characterized by single crystal X-ray diffraction, elemental analyses, IR and magnetic investigation. Complex **1**·H_2O·$3CH_3CN$ crystallizes in the monoclinic space group *I*2/*a* and its core can be viewed as a Mn_6 hexagon of alternating Mn^{II} and Mn^{III} ions surrounding a central Mn^{III} ion, which has previously not been seen for this topology. Magnetic studies reveal that overall ferromagnetic coupling between Mn^{III} and Mn^{II} or Mn^{III} ions within **1**·H_2O are present and weak frequency dependence of the ac-susceptibility was found. CCDC: 1045766.

Keywords: heptanuclear Mn complex; mixed-chelating ligand; multidentate chelating ligand; crystal structure; magnetic property

Since the discovery of slow magnetization relaxation for [$Mn_{12}O_{12}(O_2CMe)_{16}(H_2O)_4$] in 1993, single molecule magnets (SMMs) have received great attention in the field of coordination chemistry because of their unique and intriguing properties and their potential applications in high-density information storage, quantum computing and molecular spintronics[1-2]. Up to date, polynuclear 3*d* transition metal complexes (especially polynuclear Mn clusters)[3-4], 3*d*-4*f* mixed-metal complexes[5-6], polynuclear pure lanthanide

收稿日期:2015-09-02。收修改稿日期:2015-11-04。

国家自然科学基金(No.21201136)和武汉工程大学科学研究基金(No.K201447)资助项目。

*通信联系人。E-mail:wangch198201@163.com,zhiqpan@163.com;会员登记号:S06N3619M1308。

clusters[7] and mononuclear *f*-based (including acitinide) or 3*d* transition metal compounds[8-10] have been reported by scientists all over the world. Nonetheless, we consider that the polynuclear 3*d* clusters, especially polynuclear Mn clusters, should not be ignored because it is important for better understanding of magnetic interactions between paramagnetic ions, the quantum tunneling of the magnetization and the mechanisms for slow magnetic relaxation.

Choosing appropriate multidentate chelating ligands is vitally important for obtaining the above types of SMMs. At early stage, carboxylate ligands have been widely used in the construction of 3*d* clusters. However, in recently years, non-carboxylate ligands have been received more attention. These non-carboxylate ligands mainly include[11]: (i) alcohol/alkoxide -based chelating ligands, such as 2-(hydroxymethyl) pyridine (hmpH)[12], 2,6-pyridinedimethanol ($pdmH_2$)[13], the gem-diolate form of di-2-pyridyl ketone ($dpkd^{2-}$)[14], 1,1,1-tris (hydroxymethyl)ethane ($thmeH_3$)[15]; (ii) polydentate Schiff-base ligands, such as *N*,*N*′-2,2-dimethylpropylenedi (3-methoxysalicylideneiminato)[16], (*E*)-2,2′-(2-hydroxy-3-((2-hydroxyphenylimino)methyl)-5-methylbenzylazanediyl)-diethanol[17]; (iii) other N- and O-based chelating ligands, such as methyl-2-pyridyl ketone (mpkoH)[18], 2, 6-diacetylpyridine dioxime ($dapdoH_2$)[19], salicylaldoxime and its derivatives (H_2salox and R-H_2salox)[20]. By detailed investigation on these multidentate chelating ligands, we found that their symmetry are different, for example, $pdmH_2$ and $thmeH_3$ possess C_2 and C_3 symmetry axes, respectively, while hmpH, mpkoH and others have no symmetry axes. Additionally, the coordinate modes of these multidentate chelating ligands are different from each other. Therefore, novel structural complexes with distinctive magnetic properties compared with complexes containing single multidentate chelating ligand may be obtained by mixing two or more kinds of ligands possessing different symmetry in a solution containing magnetic spin carrier salts. Actually, we have obtained [Mn_4], [Mn_{13}] and [Mn_{16}] clusters containing mixed chelating ligands[21-22]. We have also found that the core structures of the tetranuclear Ni clusters can be transformed from a defect dicubane-like core to a cubane-like core by adding of auxiliary multidentate chelating ligand of 2-(hydroxymethyl) pyridine ligands[23]. As a part of our continuing studies on the synthesis and magnetic properties of SMMs clusters containing mixed multidentate chelating ligands, we report herein a heptanuclear Mn cluster, namely $[Mn^{II}_3Mn^{III}_4(Cl)_6(hmp)_6(thme)_2]\cdot H_2O\cdot 3CH_3CN$ (**1**$\cdot H_2O\cdot 3CH_3CN$). Magnetic studies reveal that overall ferromagnetic coupling between Mn^{III} and Mn^{II} or Mn^{III} ions within complex **1**$\cdot H_2O$ are present and weak frequency dependence of the ac-susceptibility was found.

1 Experimental

1.1 Materials and measurements

All the starting materials for synthesis were commercially available and used as received. Elemental analyses for C, H and N were carried out using an Elementar Vario Perkin-Elmer 240C analyzer. IR spectra were obtained at room temperature using KBr pellets in the range of 4 000~400 cm^{-1} on a VECTOR 22 spectrometer. Magnetic measurements on crystalline samples were performed on a Quantum Design MPMS-XL7 superconducting quantum interference device (SQUID) magnetometer. The direct current (dc) measurements were collected at an applied field of 2 kOe and from 1.8 to 300 K, and the alternating-current (ac) measurements were carried out in a 5.0 Oe ac field oscillating at various frequencies from 1 to 1 500 Hz and without dc field. The diamagnetic corrections for the compounds were estimated using Pascal′s constants, and magnetic data were corrected for diamagnetic contributions of the sample holder.

1.2 Preparation of $[Mn^{II}_3Mn^{III}_4(Cl)_6(hmp)_6(thme)_2]\cdot H_2O\cdot 3CH_3CN$ (1$\cdot H_2O\cdot 3CH_3CN$)

A mixture of $MnCl_2\cdot 4H_2O$ (0.082 5 g, 0.4 mmol), 1,1,1-tris(hydroxymethyl)ethane (0.049 4 g, 0.4 mmol), 2-pyridinemethanol (0.045 5 g, 0.4 mmol), triethylamine (0.126 g, 1.2 mmol) in a molar ratio of 2:1:2:2:6 in CH_3CN was stirred at room temperature for half an hour, forming a red-orange solution from which brown

crystals of the compounds **1**·H_2O·$3CH_3CN$ were formed after several days. Yield: 0.032 5 g (38% based on Mn). It should be noted that, for complex **1**·H_2O·$3CH_3CN$, vacuum-drying has resulted in three MeCN solvent molecules free. Anal. Calcd. for **1**·H_2O($C_{46}H_{56}Cl_6Mn_7N_6O_{13}$,%): C, 36.88; H, 3.77; N, 5.61. Found (%): C, 36.78; H, 3.68; N, 5.57. IR (KBr, cm^{-1}): 3 422 (s), 2 872 (m), 1 605 (m), 1 522 (m), 1 460 (m), 1 384 (m), 1 122 (w), 1 047 (s), 915 (w), 763 (w), 582 (m).

1.3 X-ray crystallography

For compound **1**·H_2O·$3CH_3CN$, the framework of single crystal samples was collapsed in the air a few minutes later, so the suitable single crystal of **1**·H_2O·$3CH_3CN$ was located in a silica tube to collect crystallographic data. Diffraction data were collected on a Bruker Smart CCD area-detector diffractometer with Mo $K\alpha$ radiation (λ=0.071 073 nm) by ω-scan mode operating at room temperature. The collected data were reduced with SAINT[24], and semi-empirical absorption correction was applied to the intensity data using the SADABS program[25]. The structure was solved by direct methods, and all non hydrogen atoms were refined anisotropically by least squares on F^2 using the SHELXTL program[26]. Hydrogen atoms were placed in calculated positions and refined isotropically using the riding model. Unit cell data and structure refinement details are listed in Table 1.

CCDC: 1045766.

Table 1 Details of the data collection and refinement parameters for 1·H_2O·$3CH_3CN$

Chemical formula	$C_{52}H_{65}Cl_6Mn_7N_9O_{13}$	Absorption coefficient	1.599
Formula weight	1 621.41	F(000)	6 568
T / K	293(2)	Crystal size / mm	0.18×0.15×0.12
Crystal system	Monoclinic	θ range (°)	1.16~25.00
a / nm	2.113 65(16)	Limiting indices	$-23 \leqslant h \leqslant 25, -21 \leqslant k \leqslant 19, -41 \leqslant l \leqslant 41$
b / nm	1.785 34(13)	Reflections total	45 369
c / nm	3.520 8(3)	Reflections unique	11 586
β / (°)	95.154(4)	Goodness-of-fit on F^2	1.075
V / nm^3	13.232 3(18)	R_{int}	0.028 6
Z	8	R_1[a] [$I>2\sigma(I)$]	0.048 4
D_c /(g·cm^{-3})	1.628	wR_2[a] (all reflections)	0.115 8

[a] $R_1=\sum||F_o|-|F_c||/\sum|F_o|$, $wR_2=[\sum w(|F_o^2|-|F_c^2|)^2/\sum w(|F_o^2|)^2]^{1/2}$

2 Results and discussion

2.1 Crystal structure description

Single-crystal X-ray diffraction analysis revealed that complex **1**·H_2O·$3CH_3CN$ crystallizes in monoclinic space group *I*2/*a*. The crystal structure of complex **1**·H_2O·$3CH_3CN$ is shown in Fig.1. Selected bond lengths and angles are given in Table 2. As can be seen from Fig.1, complex **1**·H_2O·$3CH_3CN$ has seven manganese atoms that are roughly in the same plane. It consists of a central $Mn^{Ⅲ}$ ion which is encircled by six Mn ions that form a roughly dislike heptanuclear Mn clusters. The outer six Mn atoms are connected with the central Mn through six μ_3-O atoms (O7, O8, O9 and O10, O11, O12) which are from $thme^{3-}$ ligands located above and below the molecular plane, respectively. As can be seen from Fig.1, **1**·H_2O·$3CH_3CN$ contains six hmp^- ligands, two $thme^{3-}$ ligands and six Cl^- terminal ligands. Each of the hmp^- ligands simultaneously binds two Mn atoms in a μ_2-η^1:η^2 fashion. Each hydroxyl O from $thme^{3-}$ coordinates with three Mn ions, and the $thme^{3-}$ ligand binds seven Mn ions in a η^3:η^3:η^3, μ_7-fashion. Oxidation-state determinations based on charge considerations and crystallographic evidences for Jahn-Teller elongated axes. It is concluded that Mn1, Mn3, Mn5, Mn7 are $Mn^{Ⅲ}$, Mn2, Mn4, Mn6 are $Mn^{Ⅱ}$. All the Mn atoms are six-coordinated with distorted octahedral geometry. For four $Mn^{Ⅲ}$ ions, each of them clearly possesses a Jahn-Teller distortion in the form of axis elongation along N2-Mn1-O7, N3-Mn3-O10, N5-Mn5-O12 and O8-Mn7-O11 (black lines in Fig.2), in which Jahn-Teller

axes for Mn1, Mn3 Mn7 are roughly parallel while these are vertical to that of Mn5. Besides, the O-Mn7-O is almost linear, with O11-Mn7-O8, O12-Mn7-O7 and O9-Mn7-O10 being 175.780°, 177.41° and

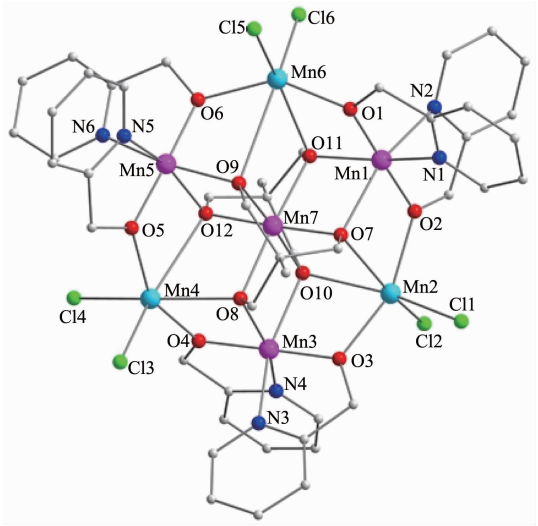

Hydrogen atoms and solvated molecules have been omitted for clarity

Fig.1 Molecular structure of complex $1 \cdot H_2O \cdot 3CH_3CN$

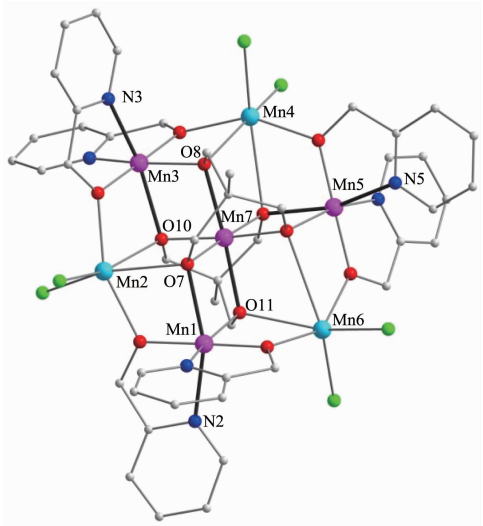

Fig.2 Black lines showing Jahn-Teller axes of Mn^{III} ions in the complex $1 \cdot H_2O \cdot 3CH_3CN$

Table 2 Selected bond lengths (nm) and bond angles (°) for $1 \cdot H_2O \cdot 3CH_3CN$

Mn1-O1	0.186 0(3)	Mn3-O8	0.208 3(3)	Mn5-O12	0.218 5(3)
Mn1-O2	0.188 6(3)	Mn3-N4	0.211 7(4)	Mn5-N5	0.218 4(4)
Mn1-O11	0.201 8(3)	Mn3-N3	0.212 6(4)	Mn6-O1	0.208 2(3)
Mn1-N1	0.208 6(4)	Mn3-O10	0.217 2(3)	Mn6-O6	0.208 7(3)
Mn1-N2	0.219 4(4)	Mn4-O5	0.212 7(3)	Mn6-O11	0.245 6(3)
Mn1-O7	0.222 7(3)	Mn4-O4	0.213 5(3)	Mn6-Cl5	0.239 27(12)
Mn2-O3	0.211 7(3)	Mn4-O8	0.232 9(3)	Mn6-Cl6	0.238 37(14)
Mn2-O2	0.213 6(3)	Mn4-Cl3	0.241 07(13)	Mn6-O9	0.287 7
Mn2-O10	0.236 0(3)	Mn4-Cl4	0.239 64(15)	Mn7-O12	0.190 6(3)
Mn2-O7	0.247 2(3)	Mn4-O12	0.267 4	Mn7-O7	0.191 8(3)
Mn2-Cl1	0.241 45(14)	Mn5-O5	0.186 5(3)	Mn7-O9	0.197 6(3)
Mn2-Cl2	0.243 84(13)	Mn5-O6	0.187 0(3)	Mn7-O10	0.200 2(3)
Mn3-O3	0.186 1(3)	Mn5-O9	0.202 8(3)	Mn7-O8	0.209 8(3)
Mn3-O4	0.186 1(3)	Mn5-N6	0.208 8(4)	Mn7-O11	0.210 4(3)

O2-Mn1-O1	97.02(12)	O3-Mn3-N4	99.59(14)	O6-Mn6-Cl5	96.52(8)
O2-Mn1-N1	99.48(13)	O4-Mn3-N4	79.87(14)	Cl6-Mn6-Cl5	107.01(5)
O11-Mn1-N1	161.30(12)	O5-Mn4-O4	151.06(11)	O1-Mn6-O11	69.32(10)
O1-Mn1-N2	100.29(13)	O5-Mn4-O8	92.33(11)	O6-Mn6-O11	88.55(10)
O3-Mn2-O10	72.95(11)	O4-Mn4-O8	71.42(11)	O7-Mn7-O11	84.26(11)
O3-Mn2-Cl1	92.52(9)	O5-Mn4-Cl4	98.58(9)	O9-Mn7-O11	91.40(11)
O2-Mn2-Cl1	99.09(9)	O5-Mn5-O9	95.21(12)	O10-Mn7-O11	92.30(11)
O10-Mn2-Cl1	158.85(8)	O6-Mn5-O9	87.79(12)	O8-Mn7-O11	176.31(11)
O3-Mn3-O4	179.19(13)	O5-Mn5-N6	96.12(13)		
O4-Mn3-O8	82.65(12)	O6-Mn5-N6	80.68(13)		

176.32°, respectively. For Mn2, Mn4 and Mn6 ions, the bond lengths of Mn-O and Mn-Cl are in the range of 0.208 3~0.287 7 nm (Mn4-O12 0.267 4 nm, Mn6-O9 0.287 7 nm) and 0.238 4~0.243 9 nm, respectively, which meet the feature of $Mn^{Ⅱ}$ ions[27].

2.2 Magnetic properties

The direct-current (dc) magnetic susceptibility measurements for polycrystalline samples of **1**·H_2O were performed between 1.8 and 300 K under an applied dc field of 2 000 Oe. The $\chi_M T$ versus T plot for **1**·H_2O was shown in Fig.3. At room temperature, the $\chi_M T$ value is 26.07 $cm^3 \cdot K \cdot mol^{-1}$, which is slightly higher than the spin-only values of 25.13 $cm^3 \cdot K \cdot mol^{-1}$ expected for three $Mn^{Ⅱ}$ and four $Mn^{Ⅲ}$ non-interacting ions. As the temperature is reduced to 30 K, the $\chi_M T$ product steadily increases to 32.46 $cm^3 \cdot K \cdot mol^{-1}$ and then drops to a value of 16.12 $cm^3 \cdot K \cdot mol^{-1}$ at 1.8 K. The χ_M values above 50 K obey the Curie-Weiss law ($\chi_M = C/(T-\theta)$) with C=24.99 $cm^3 \cdot K \cdot mol^{-1}$ and θ=13.65 K. The positive θ value and the increase in $\chi_M T$ on lowering the temperature show that the overall ferromagnetic coupling interactions between Mn ions within the cluster are present.

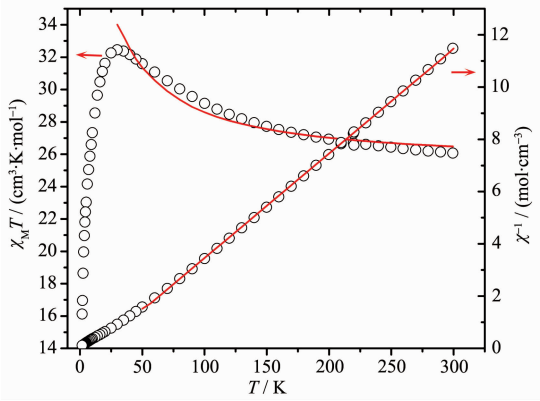

Solid lines represent the fitted results by Curie-Weiss law or by MAGPACK program[28]

Fig.3　Temperature dependence of $\chi_M T$ for **1**·H_2O

To obtain the sign and magnitude of the magnetic exchange interactions between Mn ions within the molecule of **1**·H_2O, fitting of the magnetic susceptibility data was carried out. Due to no symmetry in the complex, each distance between $Mn^{Ⅱ}$/$Mn^{Ⅲ}$ and $Mn^{Ⅲ}$ is different, so a precise fitting of the magnetic data require too many exchange constants. However, from the crystal structure, the alternative $Mn^{Ⅱ}$ and $Mn^{Ⅲ}$ atoms in the Mn_6 ring are linked by one hydroxyl group O atom of an hmp^- and one O atom of a $thme^{3-}$, and each of $Mn^{Ⅱ}$ or $Mn^{Ⅲ}$ in the Mn_6 ring is connected to the central Mn7 by two O atoms of two different $thme^{3-}$ ligands. Therefore, it is instructive to employ a simplified three-J model (Fig.4), which leads to the following Heisenberg Hamiltonian:

$$\hat{H} = -2J_1(S_{Mn1}S_{Mn2}+S_{Mn2}S_{Mn3}+S_{Mn3}S_{Mn4}+S_{Mn4}S_{Mn5}+S_{Mn5}S_{Mn6}+S_{Mn1}S_{Mn6}) - 2J_2(S_{Mn1}S_{Mn7}+S_{Mn3}S_{Mn7}+S_{Mn5}S_{Mn7}) - 2J_3(S_{Mn2}S_{Mn7}+S_{Mn4}S_{Mn7}+S_{Mn6}S_{Mn7}) \quad (1)$$

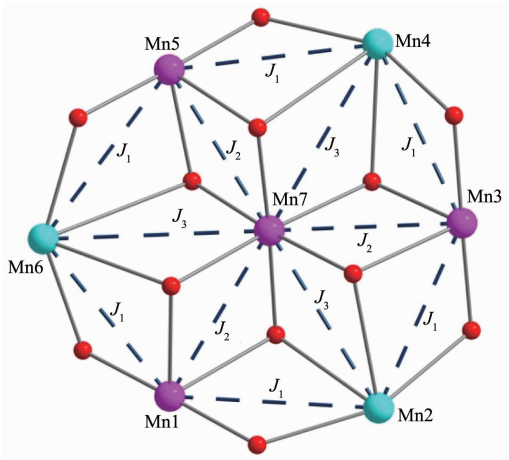

Fig.4　Model for fitting the magnetic data of **1**·H_2O

It should be noted that the above Heisenberg Hamiltonian based on the magnetic isotropic parameters, due to the dimension of full energy matrix being 135 000 for $[Mn^{Ⅱ}_3Mn^{Ⅲ}_4]$ if the magnetic anisotropic parameters were employed, which goes beyond the operating limit of our computer. The magnetic data above 30 K have been fitted by MAGPACK program[28], with the best parameters being: J_1 =−0.6 cm^{-1}, J_2 = 4.1 cm^{-1}, J_3=0.75 cm^{-1}, g=2.0 and R=4.15×10^{-4} ($R = \sum[(\chi_M T)_{obs}-(\chi_M T)_{calc}]^2/\sum(\chi_M T)_{obs}^2$). The signs of the coupling constants show that the antiferromagnetically coupling interactions are present in the Mn_6 ring, in which $Mn^{Ⅱ}$ and $Mn^{Ⅲ}$ are further antiferromagnetically and ferromagnetically coupled to the central $Mn^{Ⅲ}$ ion, respectively.

To obtain the ground-state S, g and the magnitude of the zero-field splitting (ZFS) parameter (D), magnetization data were collected in the range of 1~7 T and 1.8~5.0 K. The plot of the reduced magnetization M

versus H/T shows that the curves are not superposed (Fig.5), giving an indication of the presence of magnetic anisotropy and/or the low-lying excited states. The magnetization data were fitted using the program ANISOFIT 2.0[29], by matrix diagonalization to a model with axial ZFS (DS_z^2) and isotropic Zeeman interactions, assuming only the ground state is populated. However, an acceptable fit could not be obtained using the data collected over the whole field range. This problem widely exits in high-nuclear clusters containing Mn^{2+} ions[30], which is caused by low-lying excited states, especially if some have an S value greater than that of the ground state (in other words, these excited states are populated even at low temperatures and at low magnetic fields). This conclusion is supported by the M versus H plot (Fig. 6), in which the magnetization steadily increases upon increasing magnetic field (H) and does not show saturation.

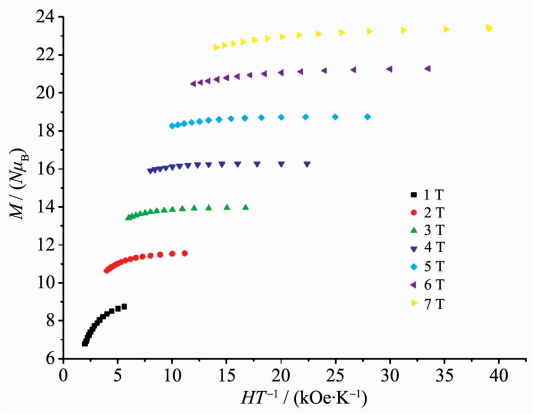

Fig.5 Plots of reduced magnetization M vs H/T for **1**·H_2O

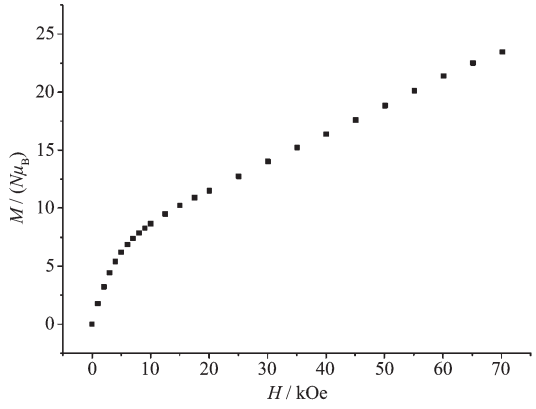

Fig.6 Plots of magnetization M vs H for **1**·H_2O

To probe the magnetization relaxation dynamics of **1**·H_2O, alternating current (ac) magnetic susceptibility data were collected in a zero-applied dc field with a 5.0 Oe ac field oscillating at frequencies in the range of 1~1488 Hz and in the temperature range of 1.8~10 K. The in-phase (χ'_M, plotted as χ'_MT) and out-of-phase (χ''_M) ac susceptibility signals are shown in Fig.7. The rapid decrease of χ'_MT with temperatures decreasing also supports a population of low-lying excited states with larger S compared to the ground-state S. Extrapolation of χ'_MT data down to 0 K gives ~22.5 $cm^3 \cdot K \cdot mol^{-1}$ [31], obtaining a ground state of $S \approx 6.5$ (Fig.8). At lower temperatures (below 2.8 K), the frequency-dependent χ''_M signals appear (Fig.7), indicating slow relaxation of the SMMs behavior. However, the peak maxima may lie at temperature below 1.8 K, which goes beyond the operating limit of our instrument. Therefore, we cannot calculate the effective energy barrier (U_{eff}) by the Arrhenius law.

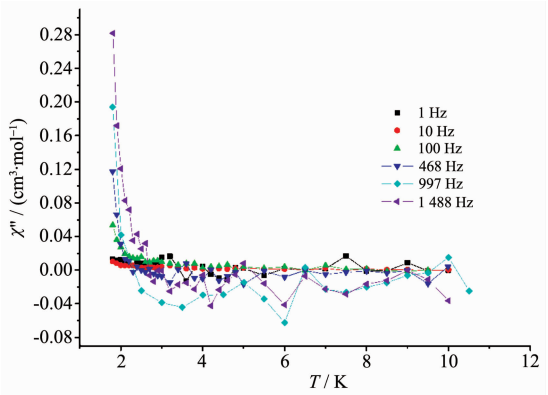

Fig.7 Plot of the temperature dependence of the out-of-phase (χ''_M) ac susceptibility signals for **1**·H_2O at the indicated frequencies

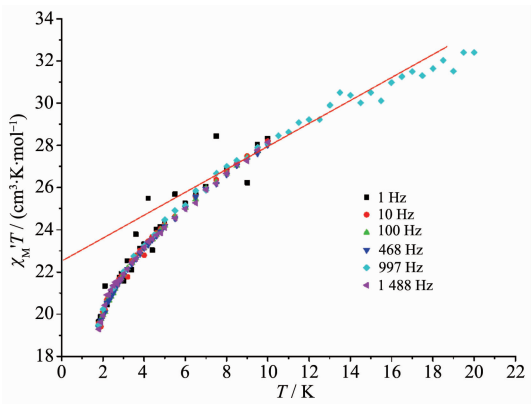

Fig.8 χ'_MT vs T plot for **1**·H_2O

2.3 Compared with other [Mn_7] clusters

It should be noted that, in the literature, there are 14 reported dislike heptanuclear Mn clusters[32], which can be classified into four categories according to their oxidation states and their distribution of the Mn ions. The first class is $Mn^{II}_4Mn^{III}_3$, in which alternating Mn^{II} and Mn^{III} ions consist of a six-member ring (Mn_6 ring) that encircles the central Mn^{II} ions. The distribution of Mn ions of the second series Mn^{II}_7 and the third class $Mn^{III}_6Mn^{II}$ (only one compound was reported), are the same as the above class, except all Mn^{III} for the former series replaced by Mn^{II} ions and Mn^{II} ions on the Mn_6 ring for the later class replaced by Mn^{III} ion, respectively. However, for the last category $Mn^{II}_3Mn^{III}_4$, the distribution of Mn ions is entirely different from the above three class, in this category, three Mn^{II} ions consist of a linear, with its either side located by two Mn^{III} ions. For **1**·H_2O·$3CH_3CN$, alternating Mn^{II} and Mn^{III} ions form a Mn_6 ring that encircles the central Mn^{III}, which is similar to that of the first class mentioned above, except the different oxidation state of the central Mn. Therefore, complex **1**·H_2O·$3CH_3CN$ represents an unprecedented oxidation state configuration, which has previously not been seen for this topology. For **1**·H_2O·$3CH_3CN$, the central Mn is coordinated to six O atoms from two $thme^{3-}$ ligands, so the change of central Mn compared to the first class may be due to the charge considerations and constraints imposed by multidentate chelating ligand $thme^{3-}$. Therefore, this paper provides a chance for changing structural configuration and/or oxidation state of polynuclear magnetic clusters by mixing two or more multidentate chelating ligands with different symmetry. Finally, it also should be noted that only a few of dislike heptanuclear Mn clusters show SMMs behaviors and **1**·H_2O·$3CH_3CN$ showing this magnetic behavior may be due to the very subtle changes of oxidation state of the central Mn.

3 Conclusions

In summary, a complex containing mixed multidentate chelating ligands with different symmetry, *i.e.* $[Mn^{II}_3Mn^{III}_4(Cl)_6(hmp)_6(thme)_2]$·$H_2O$·$3CH_3CN$ (**1**·H_2O·$3CH_3CN$), has been synthesized by the reactions of $MnCl_2·4H_2O$, hmpH and $thmeH_3$ in MeCN. For **1**·H_2O·$3CH_3CN$, alternating Mn^{II} and Mn^{III} ions form a Mn_6 ring that encircles the central Mn^{III}, and this structural topology has previously not been seen. This structural change may be due to the charge considerations and constraints imposed by multidentate chelating ligand $thme^{3-}$. Magnetic studies reveal that the overall ferromagnetic interactions between neighboring Mn atoms within **1**·H_2O are present, and weak frequency dependence of the ac-susceptibility was found, which represents a few of examples with SMMs behavior in dislike Mn_7 clusters. Finally, this work provides a chance for changing structural configuration and/or oxidation state of polynuclear magnetic clusters by mixing two or more multidentate chelating ligands with different symmetry.

References:

[1] Bagai R, Christou G. *Chem. Soc. Rev.*, **2009**,**38**:1011-1026

[2] Milios C J, Inglis R, Vinslava A, et al. *J. Am. Chem. Soc.*, **2007**,129:12505-12511

[3] Coronado E, Forment-Aliaga A, Gaita-Arino A, et al. *Angew. Chem., Int. Ed.*, **2004**,**45**:6152-6156

[4] Nicholas C H, Milissa A B, Wolfgang W, et al. *Inorg. Chem.*, **2003**,**42**:7067-7076

[5] Saha A, Thompson M, Abboud K A, et al. *Inorg. Chem.*, **2011**,**50**:10476-10485

[6] Schray D, Abbas G, Lan Y, et al. *Angew. Chem., Int. Ed.*, **2010**,**49**:5185-5188

[7] Blagg R J, Ungur L, Tuna F, et al. *Nat. Chem.*, **2013**,**5**:673-678

[8] ZHANG Lu(张璐), ZENG Su-Yuan(曾涑源), LIU Tao(刘涛), et al. *Chinese J. Inorg. Chem.*(无机化学学报), **2015**,**31**(9):1761-1773

[9] Le Roy J J, Ungur L, Korobkov I, et al. *J. Am. Chem. Soc.*, **2014**,**136**:8003-8010

[10]Zhu Y Y, Cui C, Zhang Y Q, et al. *Chem. Sci.*, **2013**,**4**:1802-1806

[11]Stamatatos T C, Christou G. *Inorg. Chem.*, **2009**,**48**:3308-3322

[12]Stamatatos T C, Poole K M, Abboud K A, et al. *Inorg. Chem.*, **2008**,**47**:5006-5021

[13]Stamatatos T C, Foguet-Albiol D, Poole K M, et al. *Inorg. Chem.*, **2009**,**48**:9831-9845

[14]Zaleski C M, Depperman E C, Dendrinou-Samara C, et al. *J. Am. Chem. Soc.*, **2005**,**127**:12862-12872

[15]Brechin E K, Soler M, Christou G, et al. *Chem. Commun.*, **2003**:1276-1277

[16]Colacio E, Ruiz J, Mota A J, et al. *Inorg. Chem.*, **2012**,**51**:5857-5868

[17]Chandrasekhar V, Bag P, Kroener W, et al. *Inorg. Chem.*, **2013**,**52**:13078-13086

[18]Stamatatos T C, Foguet-Albiol D, Lee S C, et al. *J. Am. Chem. Soc.*, **2007**,**129**:9484-9499

[19]Stamatatos T C, Luisi B S, Moulton B, et al. *Inorg. Chem.*, **2008**,**47**:1134-1144

[20]Milios C J, Vinslava A, Whittaker A G, et al. *Inorg. Chem.*, **2006**,**45**:5272-5274

[21]Wang H S, Zhang Z C, Song X J, et al. *Dalton Trans.*, **2011**, **40**:2703-2706

[22]WANG Hui-Sheng(王会生). *Chinese J. Inorg. Chem.*(无机化学学报), **2014**,**30**(3):522-528

[23]Wang H S, Song Y. *Inorg. Chem. Commun.*, **2013**,**35**:86-88

[24]*SAINT-Plus, Version* 6.02, Bruker Analytical X-ray System: Madison, WI, **1999**.

[25]Sheldrick G M. *SADABS*: *An Empirical Absorption Correction Program*, Bruker Analytica X-ray Systems: Madison, WI, **1996**.

[26]Sheldrick G M. *SHELXTL*-97, University of Göttingen, Göttingen, Germany, **1997**.

[27]Zhang Z M, Yao S, Li Y G, et al. *Chem. Commun.*, **2013**,**49**:2515-2517

[28]Borrás-Almenar J J, Clemente-Juan J M, Coronado E, et al. *Inorg. Chem.*, **1999**,**38**:6081-6088

[29]Shores M P, Sokol J J, Long J R. *J. Am. Chem. Soc.*, **2002**, **124**:2279-2292

[30]Scott R T W, Parsons S, Murugesu M, et al. *Angew. Chem., Int. Ed.*, **2005**,**44**:6540-6543

[31]Murugesu M, Habrych M, Wernsdorfer W, et al. *J. Am. Chem. Soc.*, **2004**,**126**:4766-4767

[32]Chen S Y, Beedle C C, Gan P R, et al. *Inorg. Chem.*, **2012**, **51**:4448-4457